

## Self-Folding Cavitands of Nanoscale Dimensions

Ulrich Lücking, Fabio C. Tucci, Dmitry M. Rudkevich,\* and Julius Rebek, Jr.\*

*Contribution from The Skaggs Institute for Chemical Biology and The Department of Chemistry, The Scripps Research Institute, MB-26, 10550 North Torrey Pines Road, La Jolla, California 92037*

Received May 5, 2000

**Abstract:** New types of resorcinarene-based nanoscale container molecules **2** and **3** are described. They feature reversibly folding unimolecular cavities of nanoscale dimensions and  $\sim 800 \text{ \AA}^3$  internal volume; they are among the largest synthetic unimolecular hosts prepared to date. Two seams of intramolecular hydrogen bonds, provided by 12 secondary amides, control the guest uptake and release. The hydrogen bonds resist the unfolding of the host and increase the energetic barrier to guest exchange. Exchange is slow on the NMR time scale (room temperature), and kinetically stable complexes result. The direct observation of bound species and the stoichiometry of the complexes are reported. A series of adamantyl and cyclohexyl guests **11–19** of various shapes and lengths were prepared and used to estimate the hosts' capacities. Compound **2** exists in an S-shaped conformation and its two cavities act independently; each half of host **2** formed kinetically stable complexes with either two identical or different guest molecules. The C-shaped host **3** accommodates rigid and long guests with association constants ( $K_a$ ) between  $500 \pm 50 \text{ M}^{-1}$  ( $-\Delta G^{295} = 3.6 \pm 0.1 \text{ kcal mol}^{-1}$ ) and  $270 \pm 100 \text{ M}^{-1}$  ( $-\Delta G^{295} = 3.2 \pm 0.2 \text{ kcal mol}^{-1}$ ) for adamantyl derivatives. With the more flexible and/or shorter guests, fast exchange between the free and complexed guest species was observed at room and higher temperatures (in toluene- $d_8$ ). Guest exchange rates of the new hosts are considerably faster than rates seen with typical hemicarcerplexes but slower than those of other open-ended cavitands.

## Introduction

Molecular recognition in chemistry generally involves the matching of concave shapes and surfaces of synthetic receptors to the convex shapes and surfaces of their smaller targets. The manifest destiny of this enterprise is inevitable—molecular hosts that completely surround their guests.<sup>1</sup> The earliest expressions were the “molecule-within-molecule” complexes of Cram and Collet, carcerands and cryptophanes. In these, covalent bonds define the host molecules<sup>2</sup> and trap guest molecules more or less irreversibly.<sup>3</sup> In hemicarcerands—molecules with larger portals—guests move in and out more freely, but only slowly.<sup>4</sup> The high kinetic stability of these systems allows the direct observation of reactive intermediates and the detection of new types of stereoisomerism that arise from restricted motions of molecules within the cramped quarters.<sup>5</sup> The molecular recognition involved in the covalent systems is not conducive to equilibrium measurements and the thermodynamic parameters that can be obtained from them; rather, the recognition is kinetic. Reversibly formed capsules, held together by intermolecular

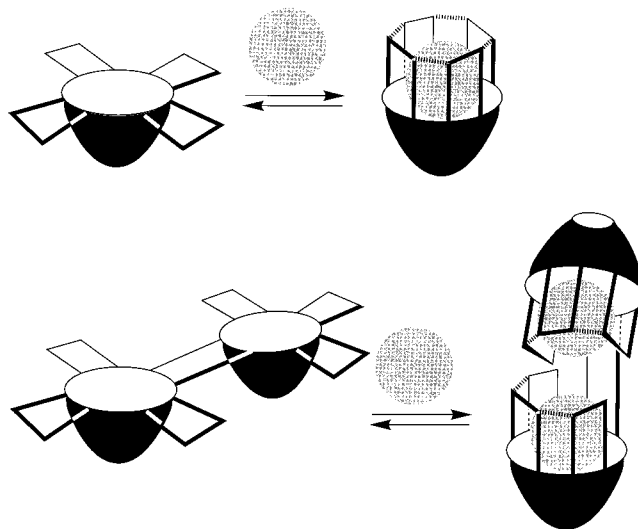


**Figure 1.** Cartoon representations of self-folding cavitands (top) and self-folding nanoscale containers (bottom), i.e., unimolecular capsules.

forces, provide one means of accomplishing recognition under equilibrium conditions and are the current vehicles, that is to say, self-assembly is the technique of choice during the past decade.<sup>6</sup> This approach gives rise to larger molecular containers that can encapsulate increasingly larger guests and incorporate the properties required for, say, catalysis. Unexpectedly, we found that even open-ended hosts, the self-folding cavitands **1**,<sup>7</sup> share some of these properties, and here we relate our latest experiences with these systems.

The key feature of these containers (Figures 1 and 2) is the conformational stability provided by their intramolecular hydrogen bonds. These bonds maintain the shape of the structure;

(1) (a) Cram, D. J.; Cram, J. M. *Container Molecules and their Guests*; Royal Society of Chemistry: Cambridge, 1994. (b) Conn, M. M.; Rebek, J., Jr. *Chem. Rev.* **1997**, *97*, 1647–1668. (c) Rudkevich, D. M.; Rebek, J., Jr. *Eur. J. Org. Chem.* **1999**, 1991–2005.

(2) Higler, I.; Timmerman, P.; Verboom, W.; Reinhoudt, D. N. *Eur. J. Org. Chem.* **1998**, 2689, 9–2702.

(3) (a) Jasat, A.; Sherman, J. C. *Chem. Rev.* **1999**, *99*, 931–967. (b) Collet, A.; Dutasta, J.-P.; Lozach, B.; Canceill, J. *Top. Curr. Chem.* **1993**, *165*, 103–129.

(4) (a) Cram, D. J.; Tanner, M. E.; Knobler, C. B. *J. Am. Chem. Soc.* **1991**, *113*, 7717–7727. (b) Cram, D. J.; Blanda, M. T.; Paek, K.; Knobler, C. B. *J. Am. Chem. Soc.* **1992**, *114*, 7765–7773. (c) Robbins, T. A.; Knobler, C. B.; Bellow, D. R.; Cram, D. J. *J. Am. Chem. Soc.* **1994**, *116*, 111–122. (d) Slow decomplexation at 295 K: Cram, D. J.; Jaeger, R.; Deshayes, K. *J. Am. Chem. Soc.* **1993**, *115*, 10111–10116.

(5) (a) Cram, D. J.; Tanner, M. E.; Thomas, R. *Angew. Chem., Int. Ed. Engl.* **1991**, *30*, 1024–1027. (b) Warmuth, R. *Angew. Chem., Int. Ed. Engl.* **1997**, *36*, 1347–1350. (c) Warmuth, R.; Marvel, M. A. *Angew. Chem., Int. Ed. Engl.* **2000**, *39*, 1117–1119. (d) Timmerman, P.; Verboom, W.; van Veggel, F. C. J. M.; van Duynhoven, J. P. M.; Reinhoudt, D. N. *Angew. Chem., Int. Ed. Engl.* **1994**, *33*, 2345–2348.

(6) (a) Rebek, J., Jr. *Acc. Chem. Res.* **1999**, *32*, 278–286. (b) de Mendoza, J. *Chem. Eur. J.* **1998**, *4*, 1373–1377. (c) Rebek, J., Jr. *Chem. Commun.* **2000**, 637–643. See also ref 1b,c.

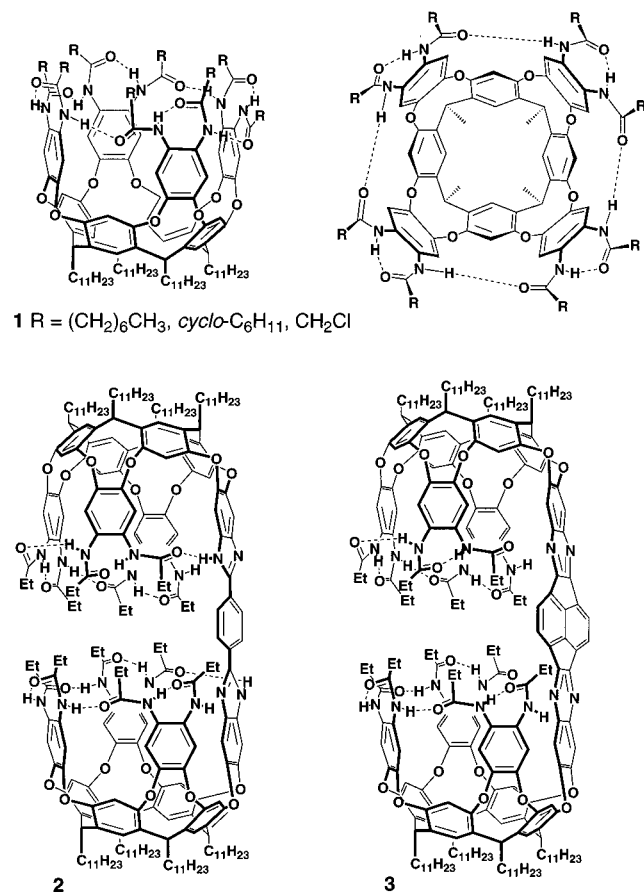


**Figure 2.** Self-folding cavitand **1**<sup>7</sup> (side and top views, only one cycloenantiomer is depicted) and self-folding containers **2** and **3**.

the deep cavities for guest inclusion result. The uptake and release of guests involves folding and unfolding of the host, achieved by varying either solvent polarity and/or temperature. The hydrogen bonds at the upper rim resist the unfolding of the vaselike structure and increase the energetic barrier to guest exchange. Accordingly, exchange is slow on the NMR time scale (ambient temperatures and 600 MHz), and kinetically stable complexes result. While the stability criterion is relative, the slow exchange permits direct observation of included species, their orientation in the cavity, and determination of the stoichiometry of the complexes.<sup>7,8</sup> The hosts have been further elaborated to self-complementary systems.<sup>9,10</sup>

The synthesis and characterization of nanoscale cavitands is the present subject and the specific structures are **2** and **3** (Figure 2). They consist of two deepened, self-folding cavitands covalently connected through an extended aromatic spacer. These are among the largest of synthetic unimolecular hosts,<sup>11</sup> featuring cavity dimensions of  $\geq 20 \times 10 \text{ \AA}$  and an internal volume of  $\sim 800 \text{ \AA}^3$ . At first glance, the molecules resemble hemicarcerands, but the dynamic qualities mentioned above offer facile access to the cavity under ambient conditions; they also accommodate guests of nanoscale dimensions and, as we shall see, more than one guest at a time.<sup>12</sup>

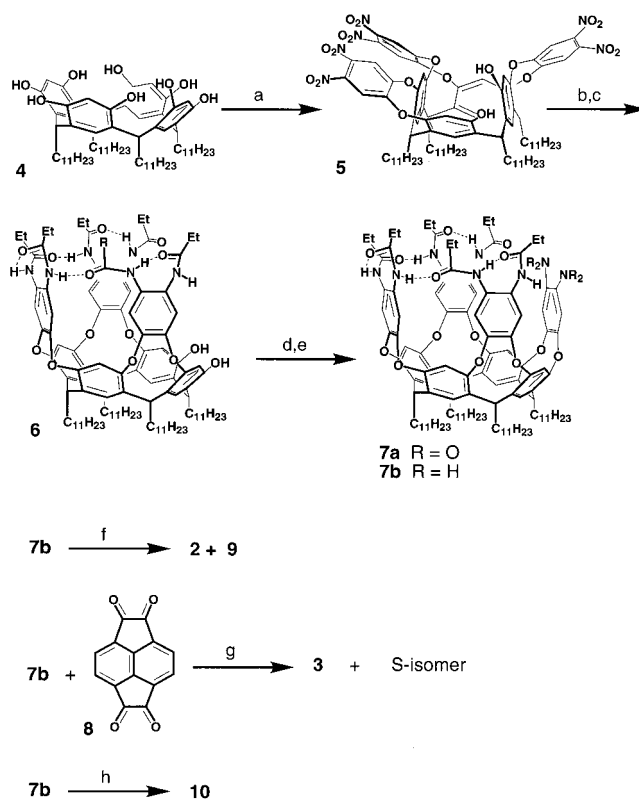
(7) (a) Rudkevich, D. M.; Hilmersson, G.; Rebek, J., Jr. *J. Am. Chem. Soc.* **1998**, *120*, 12216–12225. (b) Rudkevich, D. M.; Hilmersson, G.; Rebek, J., Jr. *J. Am. Chem. Soc.* **1997**, *119*, 9911–9912.

(8) Ma, S.; Rudkevich, D. M.; Rebek, J., Jr. *Angew. Chem., Int. Ed. Engl.* **1999**, *38*, 2600–2602.

(9) (a) Renslo, A. R.; Rudkevich, D. M.; Rebek, J., Jr. *J. Am. Chem. Soc.* **1999**, *121*, 7459–7460. (b) Renslo, A. R.; Tucci, F. C.; Rudkevich, D. M.; Rebek, J., Jr. *J. Am. Chem. Soc.* **2000**, *122*, 4573–4582.

(10) Saito, S.; Rudkevich, D. M.; Rebek, J., Jr. *Org. Lett.* **1999**, *1*, 1241–1244.

### Scheme 1<sup>a</sup>



(a) 1,2-Difluoro-4,5-dinitrobenzene (3 equiv), Et<sub>3</sub>N (16 equiv), DMF, 70 °C, 16 h, 57%. (b) Ra/Ni, H<sub>2</sub>, toluene/MeOH, 3:1, 40 °C, 12 h, >90%. (c) C<sub>2</sub>H<sub>5</sub>C(O)Cl (~10 equiv), Py (18 equiv), CH<sub>2</sub>Cl<sub>2</sub>, -78 °C, 1 h. Then NH<sub>2</sub>NH<sub>2</sub>/H<sub>2</sub>O (10 equiv), nitrobenzene, 140 °C, 24–36 h, 52%, or C<sub>2</sub>H<sub>5</sub>C(O)Cl (~10 equiv), K<sub>2</sub>CO<sub>3</sub> (20 equiv), EtOAc/H<sub>2</sub>O, then NH<sub>2</sub>NH<sub>2</sub>/H<sub>2</sub>O (10 equiv), toluene/EtOH, 1:1, 85 °C, 4.5 h, 66%. (d) 1,2-Difluoro-4,5-dinitrobenzene (2 equiv), Et<sub>3</sub>N (10 equiv), DMF, 70 °C, 15 h, 65%. (e) Ra/Ni, H<sub>2</sub>, toluene, 40 °C, 3 h, 65%. (f) 1,4-Diformylbenzene (0.5 equiv), nitrobenzene, 140 °C, 24–36 h, 52%. (g) 1,2,5,6-Tetraketopyracene **8** (0.5 equiv), AcOH<sub>Glac</sub>/THF, 1:100, reflux, 15 h, 55% C- + S-isomers (~1:1 ratio). (h) 1,2-Acenaphthenequinone, AcOH<sub>Glac</sub>/THF, 1:100, reflux, 3 h, 78%.

### Results and Discussion

**Synthesis** (Scheme 1). The synthesis of unimolecular containers **2** and **3** is based on the regioselective functionalization of resorcinarenes<sup>9,12</sup> and the modular deepening of cavitands.<sup>13</sup> Partial bridging of the hydroxyls in resorcinarene **4** with 1,2-difluoro-4,5-dinitrobenzene led to hexanitro derivative **5**. The NO<sub>2</sub> groups were reduced (H<sub>2</sub>, Ra/Ni, toluene) and then acylated with propanoyl chloride (Py, CH<sub>2</sub>Cl<sub>2</sub>, -78 °C, or K<sub>2</sub>CO<sub>3</sub>, EtOAc/H<sub>2</sub>O, rt).<sup>14</sup> The remaining two resorcinol hydroxyls were

(11) For other approaches toward nanosize host molecules, see: (a) Timmerman, P.; Nierop, K. G. A.; Brinks, E. A.; Verboom, W.; van Veggel, F. C. J. M.; van Hoorn, W.-P.; Reinhoudt, D. N. *Chem. Eur. J.* **1995**, *1*, 132–143. (b) Higler, I.; Timmerman, P.; Verboom, W.; Reinhoudt, D. N. *J. Org. Chem.* **1996**, *61*, 5920–5931. (c) Higler, I.; Verboom, W.; van Veggel, F. C. J. M.; de Jong, F.; Reinhoudt, D. N. *Liebigs Ann./Recueil* **1997**, 1577–1586. (d) Chopra, N.; Sherman, J. C. *Angew. Chem., Int. Ed. Engl.* **1999**, *38*, 1955–1957. (e) Chopra, N.; Naumann, C.; Sherman, J. C. *Angew. Chem., Int. Ed. Engl.* **2000**, *39*, 194–196. (f) Lützen, A.; Renslo, A. R.; Schalley, C. A.; O'Leary, B. M.; Rebek, J., Jr. *J. Am. Chem. Soc.* **1999**, *121*, 7455–7456. Earlier examples of unimolecular capsules: (g) Chapman, R. G.; Sherman, J. C. *J. Am. Chem. Soc.* **1998**, *120*, 9818–9826. (h) Brody, M. S.; Schalley, C. A.; Rudkevich, D. M.; Rebek, J., Jr. *Angew. Chem., Int. Ed. Engl.* **1999**, *38*, 1640–1644.

(12) Portion of this work has been published as a preliminary communication: Tucci, F. C.; Renslo, A. R.; Rudkevich, D. M.; Rebek, J., Jr. *Angew. Chem., Int. Ed. Engl.* **2000**, *39*, 1076–1079.

(13) Tucci, F. C.; Rudkevich, D. M.; Rebek, J., Jr. *J. Org. Chem.* **1999**, *64*, 4555–4559.

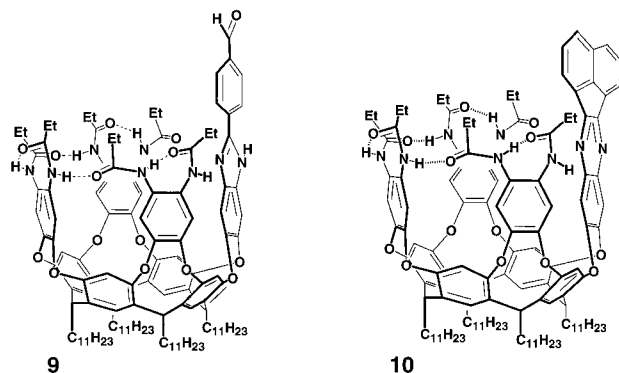


**Figure 3.** Model self-folding cavitands **9** and **10**.

also acylated under these conditions, but they were deprotected with  $\text{NH}_2\text{NH}_2$  in toluene/EtOH to give hexamide diol **6**. Reaction of **6** with another equivalent of 1,2-difluoro-4,5-dinitrobenzene produced dinitro derivative **7a**, which was readily reduced with Ra/Ni to give diamine **7b**. Heterocyclization and simultaneous oxidation<sup>15</sup> of **7b** with terephthalaldicarboxaldehyde in hot nitrobenzene as solvent and oxidant resulted in host **2** in 52% yield.

Condensation of **7b** with 1,2,5,6-tetraketopyracene **8** ( $\text{AcO-H}_{\text{glac}}/\text{THF}$ , 1:100, reflux) gave 55% of the C-shaped container **3** together with its S-shaped isomer (not shown). They were separated by chromatography. The assignment of the C- (**3**) and S-shaped diastereomers was performed through  $^1\text{H}$  NMR spectroscopy and ROESY experiments with their host-guest complexes and will be described below. Self-folding cavitands **9** and **10**, which adequately represent the structural "halves" of the hosts **2** and **3**, respectively, were also prepared and used for the model studies (Figure 3). Thus, cavitand **9** was first isolated as a byproduct in the reaction between **7b** and terephthalaldicarboxaldehyde; its synthesis was further optimized by using a larger excess of the dialdehyde. Reflux of diamine **7b** with 1,2-acenaphthenequinone ( $\text{AcOH}_{\text{glac}}/\text{THF}$ , 3 h) resulted in cavitand **10** in 78% yield. Guest molecules **11**, **12**, and **15–19** were synthesized by acylation of 1-adamantanamine and cyclohexylamine with the corresponding acid chlorides.

**Spectroscopic Properties and Conformational Analysis.** Self-folding cavitands **1** possess a vase-shaped  $C_4$  symmetrical structure of  $8 \times 10 \text{ \AA}$  dimensions.<sup>7</sup> As follows from the extensive IR and  $^1\text{H}$  and  $^{13}\text{C}$  NMR spectroscopic studies, molecular modeling, and X-ray analysis,<sup>7,8,16</sup> the upper rim of **1** features a seam of intramolecular hydrogen bonds formed by the eight secondary amide groups. Four longer intramolecular but interannular  $\text{C}=\text{O}\cdots\text{HN}$  hydrogen bonds bridge the neighboring aromatic walls; four shorter, intraannular hydrogen bonds fix the orientations of the two amides on a given *o*-phenylene-

(14) When *n*-octanoyl chloride was used as an acylating agent, the corresponding hosts, homologous to **2** and **3** (octyl-**2** and octyl-**3**), were also isolated and characterized. However, molecular modeling and also preliminary  $^1\text{H}$  NMR experiments showed that the long octyl chains result in significant steric hindrances and prevent the encapsulation processes. Moreover, in the case of the octyl-**2** compound, the alkyl chains were seen self-encapsulated within the internal cavity ( $^1\text{H}$  NMR, benzene- $d_6$  or toluene- $d_8$ , 295 K). Selected data for Octyl-**2**: Yield 41%; MALDI-MS  $m/z$  4653 avg. ( $[\text{M} + \text{H}]^+$ , calcd for  $\text{C}_{296}\text{H}_{422}\text{N}_{16}\text{O}_{28}\text{H}$  4653). Selected data for octyl-**3**: Yield 39% (C + S isomers); mp > 250 °C; MALDI-MS  $m/z$  less polar band 4717, polar band 4725 avg. ( $[\text{M} + \text{H}]^+$ , calcd for  $\text{C}_{302}\text{H}_{420}\text{N}_{16}\text{O}_{28}\text{H}$  4723.8).

(15) For the typical procedure, see: Yadagiri, B.; Lown, J. W. *Synth. Commun.* **1990**, *20*, 955–963.

(16) For further structural details (X-ray and  $^1\text{H}$  and  $^{13}\text{C}$  NMR) of self-folding cavitands **1**, including the enantiomerically pure compounds, see: Shivanyuk, A.; Rissanen, K.; Körner, S. K.; Rudkevich, D. M.; Rebek, J., Jr. *Helv. Chim. Acta* **2000**, *83*, 1778–1790.

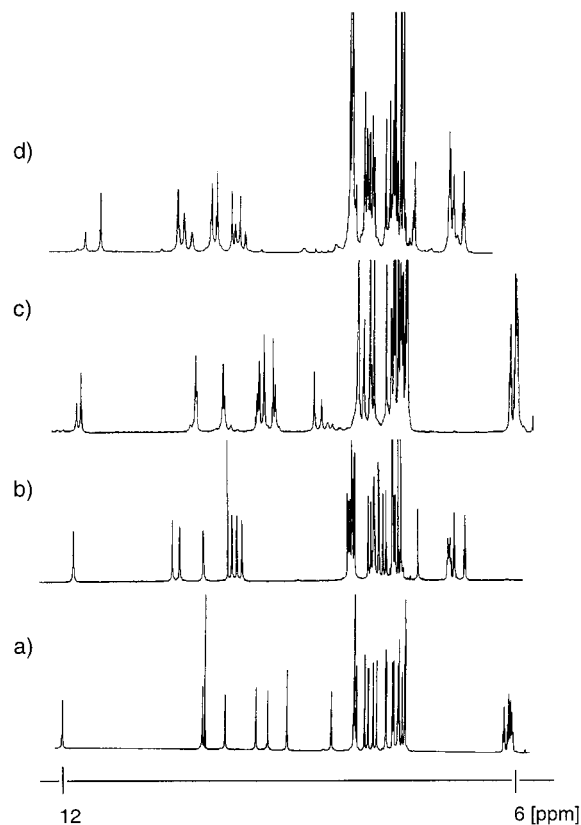


**Figure 4.** Portions of the  $^1\text{H}$  NMR spectra (600 MHz, 295 K) of (a) **9** in  $\text{CD}_2\text{Cl}_2$ , (b) **9** in toluene- $d_8$ , (c) **2** in  $\text{CD}_2\text{Cl}_2$ , and (d) **2** in toluene- $d_8$ . In the downfield region, the NH singlets are seen at 8–12 ppm. The methine CH triplets are situated at 6–6.5 ppm.

diamine unit. The head-to-tail seam results in two cycloenantiomers,<sup>17</sup> with clockwise and counterclockwise orientation of the  $\text{HN}-\text{CO}$  bonds. The interconversion between two enantiomers is slow on the NMR time scale in  $\text{CDCl}_3$  and aromatic solvents and fast in more polar acetone- $d_6$ .

The CH triplet of the methine bridge in **1** is situated downfield of 5.5 ppm at room temperature (in  $\text{CDCl}_3$  and aromatic solvents). This chemical shift is usually used to estimate the degree of the cavitand's conformational mobility; the methine shifts downfield of 5.5 ppm indicate a stable vase conformation, while shifts upfield of 4 ppm are characteristic of the  $C_{2v}$  symmetrical kite conformation.<sup>18,13</sup> The  $^1\text{H}$  NMR spectra of self-folding cavitands **9** and **10** and containers **2** and **3** also showed the spectroscopic earmarks of the vase conformation of their cavities at room temperature (in deuterated chlorinated solvents and aromatic solvents), with the characteristic methine CH signals at ~6 ppm. Moreover, the amide NH singlets are situated downfield of 8 ppm, indicating their involvement in strong hydrogen bonding (Figures 4–6).

Additional features arise from the nonsymmetrical wall arrangements of **2** and **3**. Specifically, the  $^1\text{H}$  NMR spectra of model cavitand **9** showed that the molecule has no mirror plane ( $\text{CD}_2\text{Cl}_2$ , toluene- $d_8$ ) and possesses seven different downfield

(17) Cycloenantiomerism: (a) Prelog, V.; Gerlach, H. *Helv. Chim. Acta* **1964**, *47*, 2288–2294. (b) Goodman, M.; Chorev, M. *Acc. Chem. Res.* **1979**, *12*, 1–7. (c) Yamamoto, C.; Okamoto, Y.; Schmidt, T.; Jäger, R.; Vögtle, V. *J. Am. Chem. Soc.* **1997**, *119*, 10547–10548. In agreement with the Prelog's terminology, enantiomers **1** possess the clock- and counterclockwise "directionality" of the eight secondary amide "building blocks" in an otherwise identical "distribution pattern", or the sequence or connectivity.

(18) (a) Moran, J. R.; Ericson, J. L.; Dalcanale, E.; Bryant, J. A.; Knobler, C. B.; Cram, D. J. *J. Am. Chem. Soc.* **1991**, *113*, 5707–5714. (b) Tucci, F. C.; Rudkevich, D. M.; Rebek, J., Jr. *Chem. Eur. J.* **2000**, *6*, 1007–1016.

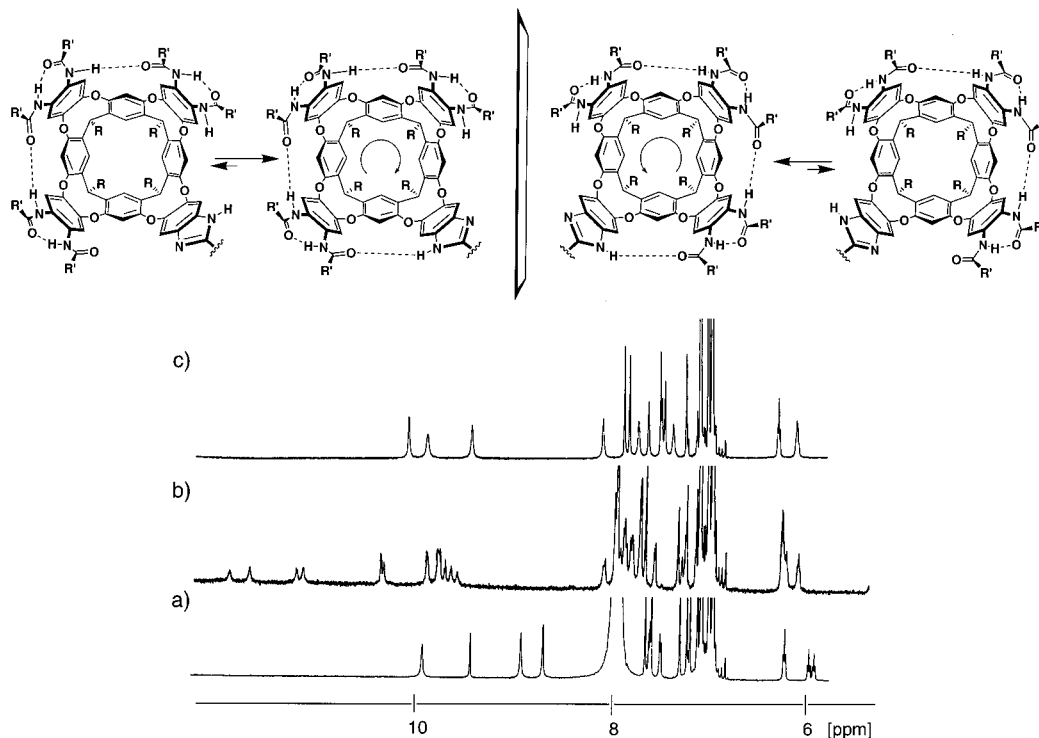


**Figure 5.** (Top) schematic representation of cycloenantiomerism and tautomerism in cavities **2** and **9**. (Bottom) portions of the  $^1\text{H}$  NMR spectra (600 MHz, 295 K) of (a) **9** in toluene- $d_8$  with 2% (vol) TFA, (b) **2** in toluene- $d_8$  with 2% (vol) DMF- $d_7$ , and (c) same as part b after addition of 2% (vol) TFA.

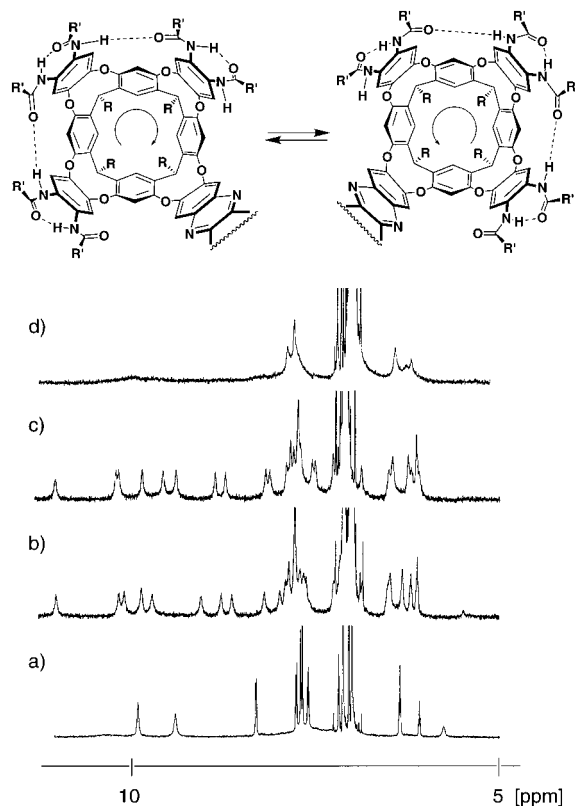


**Figure 6.** (Top) schematic representation of cycloenantiomerism in cavities **3** and **10**. (Bottom) downfield portions of the  $^1\text{H}$  NMR spectra (600 MHz, 295 K) of (a) **10** in toluene- $d_8$ , (b) **3** in toluene- $d_8$ , (c) **3** in benzene- $d_6$ , and (d) **3** in *p*-xylene- $d_{10}$ .

NH singlets (Figure 4a,b). Obviously, cycloracemization of the  $\text{C}=\text{O}\cdots\text{H}-\text{N}$  seam takes place slowly, if it takes place at all.

Since the benzimidazole NH proton is also involved, such racemization would require the tautomerization of this heterocycle. Addition of TFA ( $\sim 2\text{--}3\%$  vol) catalyzes the cycloracemization: only three amide singlets are observed (a time-averaged plane of symmetry in **9** develops and the (protonated) benzimidazole NH signals shift downfield to  $\sim 14$  ppm (Figure 5a).

The  $^1\text{H}$  NMR spectra of compound **2** are sharp in benzene- $d_6$ , toluene- $d_8$ ,  $\text{CD}_2\text{Cl}_2$ , and  $\text{CDCl}_3$  at room temperature (Figure 4c,d). From molecular modeling and also by analogy with cavitand **9** (Figure 7), the  $\text{C}(\text{O})-\text{NH}$  amides of each cavitand form a seam of five intramolecular hydrogen bonds within a vase-like structure, and the additional hydrogen bond is formed between the benzimidazole NH and its neighboring  $\text{C}=\text{O}$  oxygen. Each cycloenantiomeric cavitand in **2** possesses either clockwise or counterclockwise arrangements of the head-to-tail amides. Indeed, two cyclodiastereomers of **2** are now clearly observed in  $\sim 1:2$  ratio; multiple NH and aromatic CH resonances are seen as two nonequal sets in the  $^1\text{H}$  NMR spectra (Figure 4c,d). The origin of this diastereoselection is presently unknown. Addition of competitive DMF- $d_7$  ( $\sim 2\text{--}3\%$  vol) did not accelerate the interconversion between the diastereomers of **2** (Figure 5b). The reason for this is that the  $-\text{NH}-\leftrightarrow=\text{N}-$  tautomerism of the benzimidazole wall is still slow in the absence of a proton source. Addition of TFA ( $\sim 2\text{--}3\%$  vol) does accelerate this process: the mirror plane, running the long axis of structure **2**, is now established on the NMR time scale; only three amide and nine aromatic CH singlets are observed. The imidazole NH singlet is shifted toward  $\sim 14$  ppm but is now obscured by the TFA signal (Figure 5c).

The  $^1\text{H}$  NMR spectrum of cavitand **10** exhibits an average  $\text{C}_{2v}$  symmetry, as only three (broad) NH singlets and three triplets for the methine CH fragments in a 2:1:1 ratio are observed (Figure 6a). In contrast to cavitand **9**, this speaks for the fast interconversion between the two cycloenantiomeric

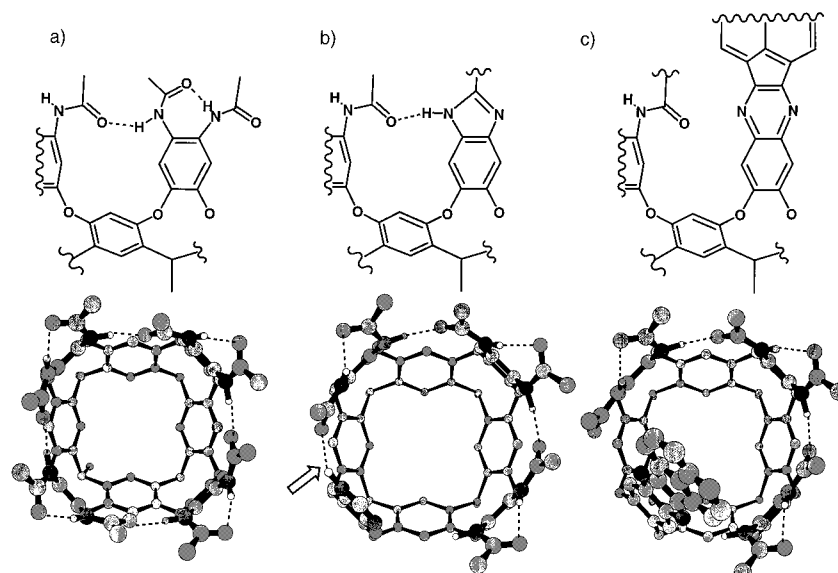


**Figure 7.** Energy-minimized structures (Amber\* force field, MacroModel 6.5 program) of self-folding cavities in (a) cavitand **1**, (b) hosts **2** and **9** (The imidazole  $N-H\cdots O=C-NH$  hydrogen bond is indicated by an arrow.), and (c) hosts **3** and **10**. The extended polycyclic wall is not involved in hydrogen bonding. Long alkyl chains and CH bonds have been omitted for viewing clarity. For all cases, only one cycloenantiomer is depicted.

forms of the amides; the extended aromatic wall in **10** is not involved in the seam of hydrogen bonds.

The  $^1H$  NMR spectra of compound **3** are relatively sharp in benzene- $d_6$  and toluene- $d_8$  but broad in *p*-xylene- $d_{10}$  at room temperature (Figure 6b–d), suggesting that the inner cavity conformation is sensitive to solvation. The NH resonances are observed downfield of 8 ppm, and the corresponding IR spectra show hydrogen-bonded NH stretching absorptions at  $3244\text{ cm}^{-1}$  (in toluene- $d_8$ ). From molecular modeling and also by analogy with cavitands **1** and **10** (Figure 7), the secondary amides of each cavitand form a seam of five intramolecular hydrogen bonds within a vaselike structure. Multiple amide NH resonances in the  $^1H$  NMR spectra of **3** indicate that two cycloenantiomers are also formed; no diastereoselectivity is observed in this case. In deuterated aromatic solvents (e.g. benzene and toluene) at least 10 equal NH singlets are seen downfield of 8 ppm, while 12 are expected for two diastereomers undergoing slow exchange. Since one amide NH in each of the cavitand subunits does not participate in the cyclic arrays, these signals appear upfield, in the aromatic region of the spectrum.

**Host–Guest Properties.** Large, nanoscale host molecules rarely show kinetically stable complexes.<sup>11a–d,f</sup> This is because large holes in their structures permit fast entry and exit of solvents and most guests to occur. The corresponding NMR chemical shift changes describe an average of the guest's many environments. For **2** and **3** kinetically stable complexes did form, even though the seam of hydrogen bonds around the rim of the structures was incomplete.

The internal diameter of unimolecular cavities **2** and **3** was reasonably estimated by comparison with self-folding cavitand **1**<sup>7,16</sup> and is  $\sim 9\text{--}10\text{ \AA}$ . The internal length of  $\sim 18\text{--}20\text{ \AA}$  was estimated from molecular modeling (Figure 8) and also experimentally, using a series of molecular rulers<sup>19</sup> (**11–19**), i.e., guest molecules of well-defined length and shape. Their dimensions are shown in Figure 9. In molecule **2** two cavities can freely rotate with respect to each other, but host **3** is rigid. By analogy with self-folding cavitands **1**,<sup>7</sup> it was anticipated that adamantyl- and cyclohexyl-containing molecules **11–19** would be the

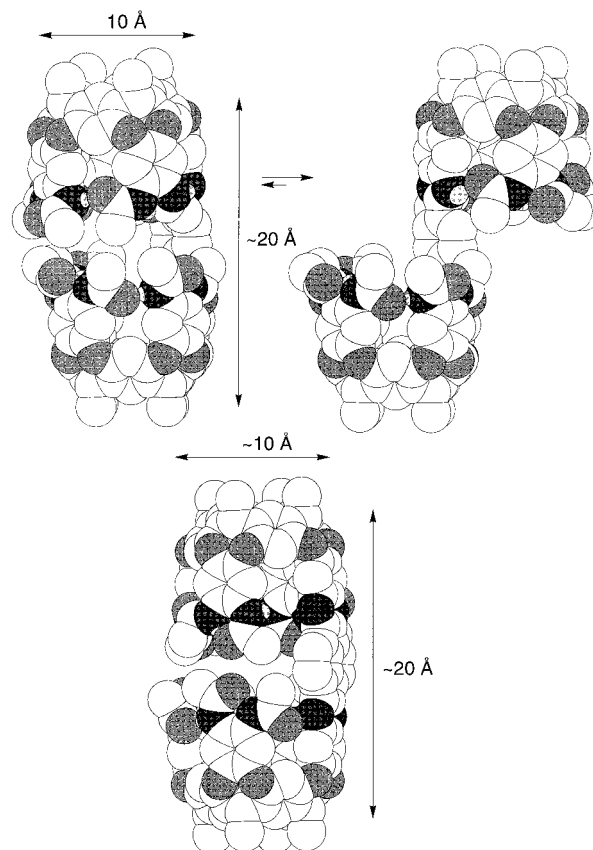


**Figure 8.** Energy-minimized structures (Amber\* force field, MacroModel 6.5 program) of self-folding nanoscale hosts **2** (top, C- and S-shaped structures) and **3** (bottom). Long alkyl chains and CH bonds have been omitted for viewing clarity.

appropriate guest species for the inner space in cavitands **9**, **10**, **2**, and **3**.

Upon complexation with **11–19** the  $^1H$  NMR spectra of hosts **2**, **3**, **9**, and **10** do undergo the expected changes (Figure 10). Integration clearly indicates the 1:1 stoichiometry for the complexes of model cavitand **9** with guest molecules **11**, **12**, **14**, **16–18**; the NMR signals of the accommodated inside guests

(19) Concept of molecular rulers: Körner, S. K.; Tucci, F. C.; Rudkevich, D. M.; Heinz, T.; Rebek, J., Jr. *Chem. Eur. J.* **2000**, *6*, 187–195.

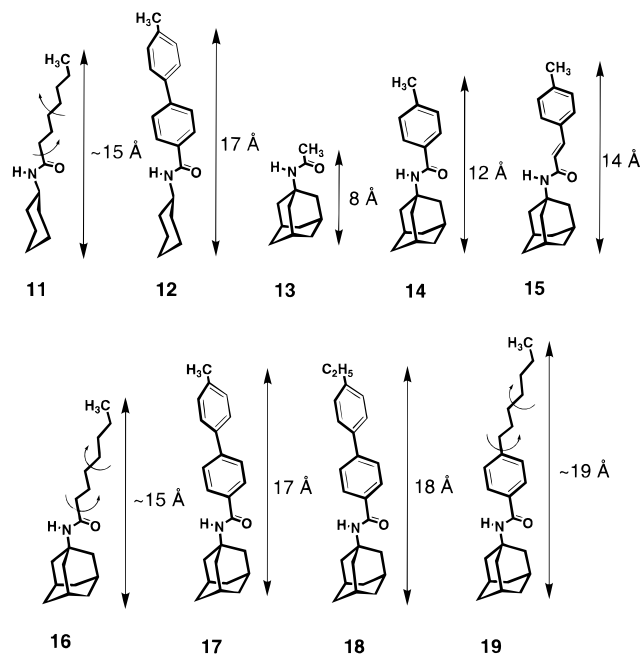


Figure 9. Guests 11–19 and their calculated dimensions.

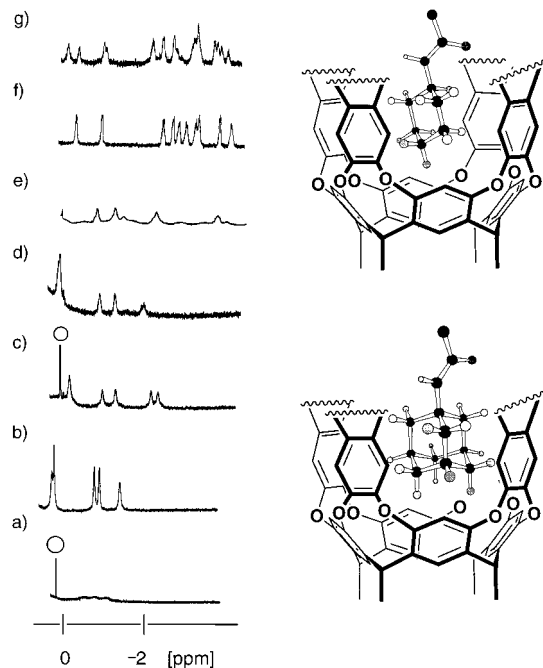


Figure 10. Encapsulation of adamantanes and cyclohexanes. Upfield portions of the  $^1\text{H}$  NMR spectra of the complexes (600 MHz, toluene- $d_8$ ) (a) **15**·**10** at 295 K, (b) **15**·**10** at 220 K (In the downfield region, all six NH singlets of cavitant **10** are clearly seen now at 8.5–11 ppm, as expected for the cyclic arrangement of the hydrogen bonds.), (c) **3**·**17** at 295 K, (d) **S**·**3**·**17** at 280 K (No upfield signals were observed at 295 K.), (e) **3**·**18** at 295 K, (f) **9**·**12** at 295 K, and (g) **12**·**2**·**12** at 295 K. (The internal standard singlet is marked as “o”.)

were seen upfield 0 ppm at room temperatures. For the complexed 1-substituted adamantanes **14**, **16**–**18**, all four signals of the skeleton protons can be clearly seen inside host **9** between 0 and –2 ppm. For the complexed cyclohexanes **11** and **12**, at least 10 multiple signals—for each CH proton of the cyclohexyl fragment—are seen inside between 0 and –3 ppm (Figure 10f). This, once again, is because the inner environment of the cavity is chiral when cycloracemization of the amides is slow. The functional group at the cyclohexane or adamantane

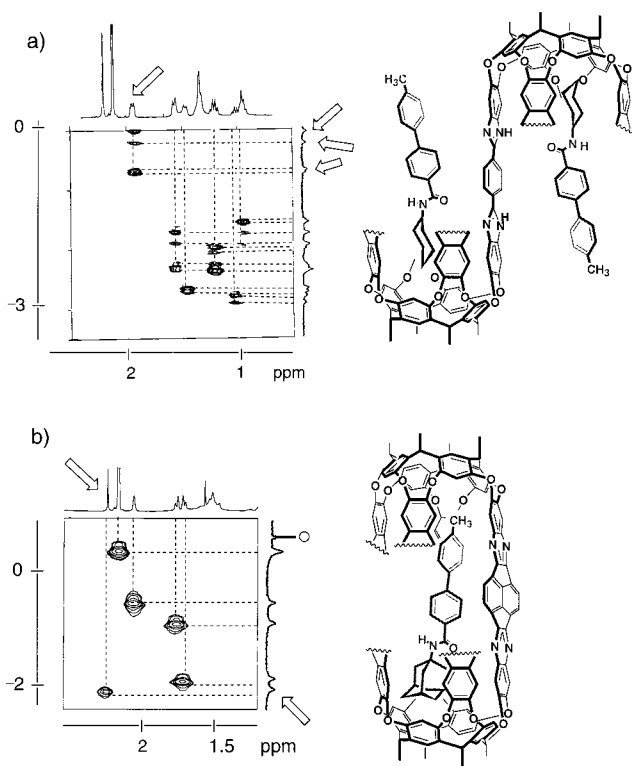


Figure 11. Fragments of the ROESY spectra (toluene- $d_8$ , 295 K) of (a) **12**·**2**·**12** [Selected exchangeable cyclohexyl CH resonances of free and encapsulated species **12** are indicated. The exchange cross-peaks for the  $\text{CH}_3$ –aryl signal (at  $\sim 2.2$  ppm) and for the aromatic portion of guest **12** are absent. Two diastereomeric complexes **12**·**2**·**12** are seen.] and (b) **3**·**17**. [The exchange cross-peaks for the  $\text{CH}_3$ –aryl signal (at  $\sim 2.2$  ppm, indicated by an arrow), aromatic portion, and adamantyl resonances of free and encapsulated guest **17** are present. The internal standard singlet is marked as before.]

1-position is generally not shifted upfield in the NMR spectra: only the cyclohexane and the adamantane skeleton is oriented toward the bottom of the cavity **9** and the functional group toward the top. The upper limit of the association constant values  $K_{\text{ass}}$  of  $\sim 80 \text{ M}^{-1}$  ( $-\Delta G^0 \sim 2.5 \text{ kcal mol}^{-1}$ ) was estimated for guests **11**, **12**, **14**, **16**–**18** directly from the integration of the corresponding  $^1\text{H}$  NMR spectra at 295 K in toluene- $d_8$ .

As was the case with **9**, host **2** gave upfield  $^1\text{H}$  NMR signals between 0 and –3 ppm on complexation with adamantane and cyclohexane guests (for example, Figure 10g). However, in host **2**, two guest molecules **11**, **12**, **14**, **16**–**18** were detected by integration inside the host's inner space, a stoichiometry not anticipated for such long guests by molecular modeling. The ROESY spectrum (Figure 11a) of the **12**·**2**·**12** complex showed the exchange cross-peaks only between the signals of the complexed cyclohexyl moiety of **12** with the signals for free **12** but not for the aromatic portion of the guest. This implies that the molecule **2** does not wrap around both ends of the guest in a C-shaped structure but rather possesses an S-shape with two cavities acting independently (Figure 12).

For the complexed cyclohexanes **11** and **12**, doubled multiple sets, for each CH proton of the cyclohexyl fragment, were detected between 0 and –3 ppm (Figure 10g). Now in addition to the chiral environment, two diastereomeric complexes are formed. This was further confirmed by the ROESY spectrum of **12**·**2**·**12** where two sets of the encapsulated cyclohexyl fragments were clearly seen (Figure 11a).

In a competition  $^1\text{H}$  NMR experiment between the bis-adamantane complex **16**·**2**·**16** and cyclohexane guest **12** in

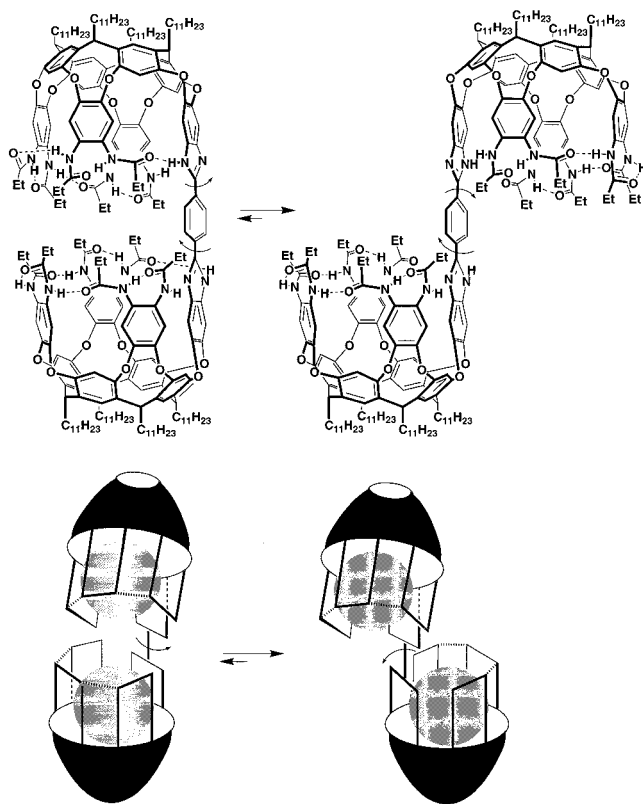


**Figure 12.** Rotational features in host **2**.

toluene-*d*<sub>8</sub>, three different complexes were observed in a roughly statistical ratio. Since the chemical shifts for the homomeric complexes **16**·**2**·**16** and **12**·**2**·**12** were known (Figure 13a,b), the signals for the heteromeric complex **12**·**2**·**16** can be assigned (Figure 13c). Specifically, two sets of the encapsulated adamantane signals were detected at ca.  $-1$  ppm (Figure 13c), one of each belongs to the **16**·**2**·**16** species. Further, the ROESY spectrum (Figure 13d) of the **12**·**2**·**16** complex showed the exchange cross-peaks between *both* sets of <sup>1</sup>H NMR signals of the complexed adamantyl moiety of **16** with the signals for free **16**. In short, the cooperative binding of the two cavities in host **2** has yet to be realized. On the other hand, this bis-cavitand, each half of which forms kinetically stable complexes with two different guests,<sup>20</sup> shows promise as a vehicle for accelerating bimolecular reactions.

In contrast to **2**, host **3** features cavities that are preorganized for cooperative binding,<sup>21</sup> and long ( $\sim 17$ – $18$  Å) rigid guests **17** and **18** readily form kinetically stable 1:1 complexes, **3**·**17** and **3**·**18**. The four adamantyl signals *and* the CH<sub>3</sub> or C<sub>2</sub>H<sub>5</sub> groups of complexed **17** and **18** were observed upfield of 0 ppm (Figure 10c–e) and assigned by ROESY experiments (Figure 11b).

These observations lay at the heart of the assignment of C-shaped **3** and distinguished it from its S-shaped (S-**3**) diastereomer. Only the adamantyl signals were seen for the complex S-**3**·**17** and also for the model complex **10**·**17**. Association constants ( $K_a$ ) of  $500 \pm 50$  M<sup>-1</sup> ( $-\Delta G^{295} = 3.6 \pm$

$0.1$  kcal mol<sup>-1</sup>) and  $270 \pm 100$  M<sup>-1</sup> ( $-\Delta G^{295} = 3.2 \pm 0.2$  kcal mol<sup>-1</sup>) were calculated for the 1:1 complexes **3**·**17** and **3**·**18**, respectively. These are an order of magnitude higher than seen for the complexes of **1** with related adamantanes.<sup>7</sup>

With the more flexible guest **16** and/or shorter ( $< 14$  Å) adamantanes **13**–**15** (Figure 9), slow exchange between the free and complexed guest species was observed only at temperatures  $< 280$  K (toluene-*d*<sub>8</sub>). For the complex **3**·**19**, but not for S-**3**·**19**, the encapsulated *n*-(CH<sub>2</sub>)<sub>6</sub>CH<sub>3</sub> signals of **19** were detected at temperatures  $\leq 240$  K in toluene-*d*<sub>8</sub>. In short, from the NMR measurements with molecular rulers **17**–**19** and by comparison with the dimensions of self-folding cavitand **1**,<sup>7,16</sup> the inner-space dimensions of host **3** of  $\sim 9 \times 18$  Å were reasonably estimated.

The ROESY spectrum of complex **3**·**17** gave an estimate for the guest exchange rate constant of  $k \sim 0.5 \pm 0.3$  s<sup>-1</sup> at 295 K.<sup>22</sup> This rate is considerably faster than exchange in Cram's hemicarceplexes with sizable guests at higher temperatures ( $k \leq 1 \times 10^{-2}$  s<sup>-1</sup>,  $\geq 373$  K)<sup>3,4</sup> but slower than that of the open-ended cavitand **1** ( $k \sim 2 \pm 1$  s<sup>-1</sup> at 295 K).<sup>7,23</sup>

**Mechanistic Considerations.** The guest exchange rate is governed by the intramolecular hydrogen bonds at the rim of structures of **2** and **3**. When these are disrupted, as on addition of DMF-*d*<sub>7</sub> to toluene-*d*<sub>8</sub> solutions of the complexes with **2** and **3**, the upfield guest signals disappear. It is unlikely that TFA is a better guest than, say, adamantanes, but DMF is expected to compete well for the cavity. Both of these solvents also compete for the hydrogen bonds. Likewise, at temperatures  $\geq 320$  K, exchange rates with **3** become fast on the NMR time scale for all guests tested. Model cavitand **10** does not form kinetically stable complexes with adamantanes **13**–**19**, even at room temperature (see also Figure 10a,b).

Conformational changes in the hosts are unavoidable during the process of guest exchange, as openings must be created that allow for guest substitution. For self-folding cavitands **1**, it was proposed that exchange of guests takes place through an unfolding of the cavity. The seam of hydrogen bonds must be (at least partly) disrupted during this process (Figure 1).<sup>7</sup> The exchange between the free and complexed adamantane guest is  $\sim 17$  kcal mol<sup>-1</sup> at 295 K, which is almost the same as the interconversion barrier between the two amide signals.<sup>7</sup> We believe the same mechanism holds for hosts **2** and **3** (Figure 1).

Cram described two stable conformations for general cavitand structures, the vase and kite.<sup>18</sup> In the latter, the four walls are flipped outward and the cavity disappears. Instead, the extended aromatic surfaces have a strong tendency toward dimerization, a process driven by solvophobic forces. These gave rise to the velcralex structures.<sup>13,18</sup> To date, no intermediates in the vase to kite change have been detected, but they may exist: structures with one, two, or three walls flipped outward. The faster exchange of smaller guests from **3** (and **10**) hints at this possibility. Their large walls are not held in place by hydrogen bonds. These can flip open and expose the encapsulated guest

(22) The rate constant  $k$  was calculated from the measurements of the cross-peak to diagonal peak intensities and the molar fractions of the guest compound **17** undergoing exchange. See for the detailed description: (a) Perrin, C. L.; Dwyer, T. J. *Chem. Rev.* **1990**, *90*, 935–967. (b) Arvidsson, P. I.; Ahlberg, P.; Hilmersson, G. *Chem. Eur. J.* **1999**, *5*, 1348–1354.

(23) Generally, much faster ( $k \gg 2$  s<sup>-1</sup>) guest exchange processes take place for open-ended cavities and the corresponding complexes are not kinetically stable. The self-assembled dimeric capsules of calix[4]arene with benzene guest show  $k \sim 0.47$  s<sup>-1</sup> (298 K) (Mogck, O.; Pons, M.; Böhrner, V.; Vogt, W. *J. Am. Chem. Soc.* **1997**, *119*, 5706–5712), and the "tennis ball" with ethane and methane shows  $k \sim 0.5$ – $1.1$  s<sup>-1</sup> (295 K) (Szabo, T.; Hilmersson, G.; Rebek, J., Jr. *J. Am. Chem. Soc.* **1998**, *120*, 6193–6194).

(20) Pairwise selection of two different guests by a self-assembled cylindrical capsule: (a) Heinz, T.; Rudkevich, D. M.; Rebek, J., Jr. *Nature* **1998**, *394*, 764–766. (b) Heinz, T.; Rudkevich, D. M.; Rebek, J., Jr. *Angew. Chem., Int. Ed. Engl.* **1999**, *38*, 1136–1139. (c) Tucci, F. C.; Rudkevich, D. M.; Rebek, J., Jr. *J. Am. Chem. Soc.* **1999**, *121*, 4928–4929. For the very recent example from the carcerand chemistry, see ref 11e.

(21) Topologically similar bis-cavitands were reported by Cram: Cram, D. J.; Tunstad, L. M.; Knobler, C. B. *J. Org. Chem.* **1992**, *57*, 528–535. No kinetically stable complexes were detected for these hosts.

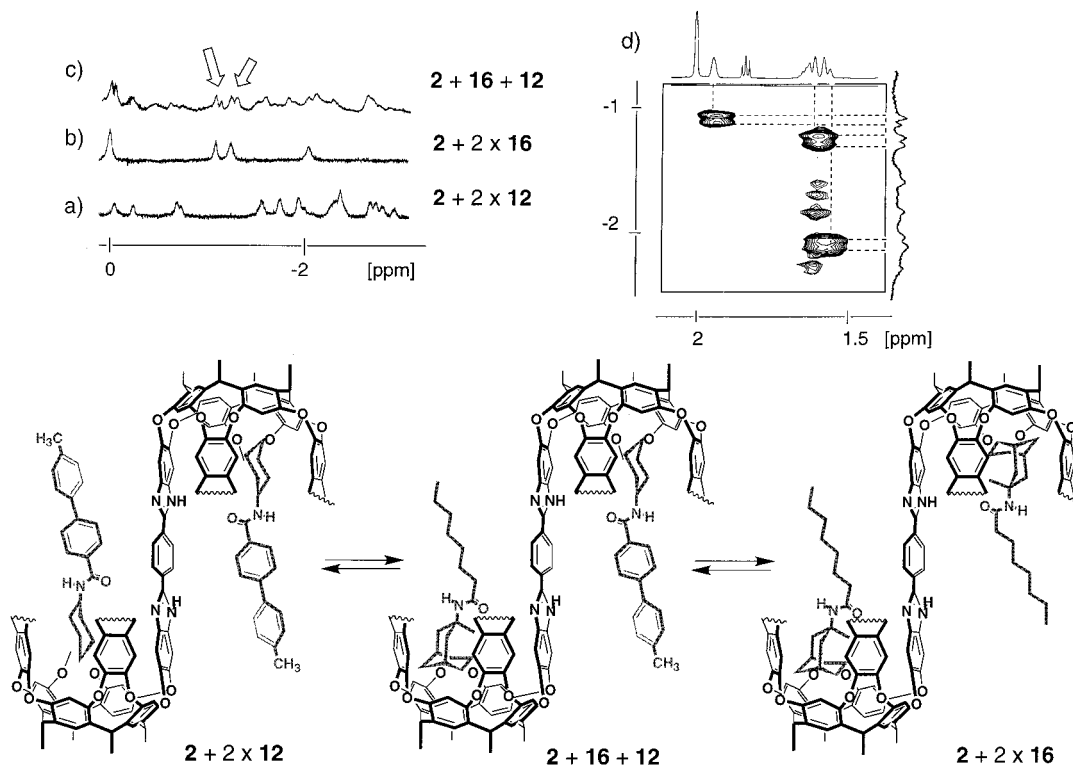


**Figure 13.** Homo-bis-caviplexes  $12 \cdot 2 \cdot 12$  and  $16 \cdot 2 \cdot 16$ , and hetero-bis-caviplex  $12 \cdot 2 \cdot 16$ . Upfield portions of the  $^1\text{H}$  NMR spectra of the complexes (600 MHz, 295 K, toluene- $d_8$ ) (a)  $12 \cdot 2 \cdot 12$ , (b)  $16 \cdot 2 \cdot 16$ , (c)  $16 \cdot 2 \cdot 16$  after addition of  $\sim 0.1$  equiv of **12** (Complex  $12 \cdot 2 \cdot 16$  emerged. Two encapsulated adamantanes are indicated by arrows.), and (d) fragment of the ROESY spectrum (toluene- $d_8$ , 295 K) of the NMR experiment c. (Two encapsulated adamantyl moieties of **16** are clearly seen in exchange with free **16**.)

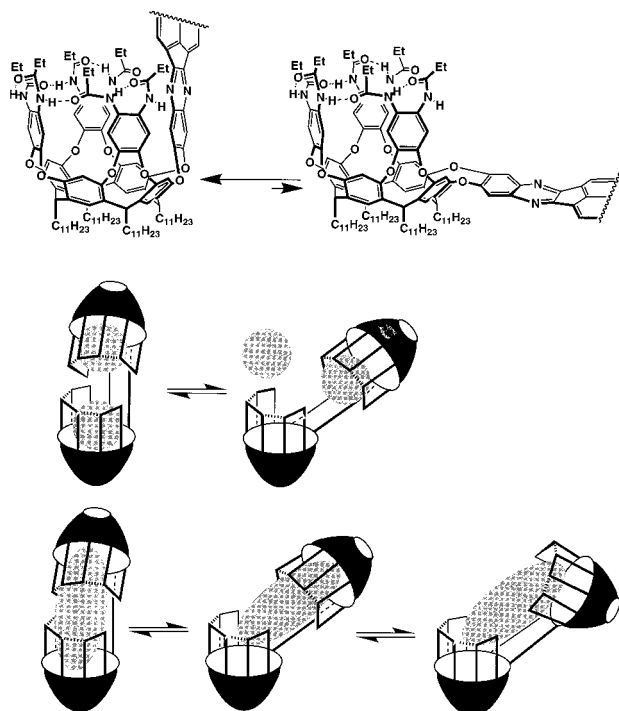


**Figure 14.** Conformational features in unimolecular capsule **3**. (Bottom) proposed mechanisms for the exchange of small and large guests in host **3**.

to displacement (Figure 14). For exchange of the longer, more rigid guests, one opening may not be enough: a second wall may have to flip out to permit substitution.

In conclusion, the self-folding containers reported here represent a new species of molecular hosts, distinct from the covalently sealed carcerands and the reversibly formed hydrogen-

bonded capsules. They are unimolecular, of nanoscale dimensions, and guest inclusion is still slow on the NMR time scale. The most immediate applications of these hosts that come to mind are as sensors for chemical analysis. A second use as reaction chambers is also intriguing: the internal space is nanoscale and the constant flow of substrates into and products out of the cavity can be imagined in the future. In the meantime, recent, concrete developments include the introduction of additional binding<sup>24</sup> and catalytically active<sup>25</sup> sites on the periphery of these structures. The synthesis of water-soluble versions for molecular recognition in aqueous solution is also underway.<sup>26</sup>

## Experimental Section

**General.** Melting points were determined on a Thomas-Hoover capillary melting point apparatus and are uncorrected.  $^1\text{H}$  NMR and  $^{13}\text{C}$  NMR spectra were recorded on Bruker AM-300 and Bruker DRX-600 spectrometers. The chemical shifts were measured relative to residual nondeuterated solvent resonances. FTIR spectra were recorded on a Perkin-Elmer Paragon 1000 PC FT-IR spectrometer. Fast Atom Bombardment (FAB) mass spectra were obtained with a VG ZAB-VSE double focusing high-resolution mass spectrometer equipped with a cesium ion gun; *m*-nitrobenzyl alcohol (NBA) was used as a matrix. High-resolution matrix-assisted laser desorption/ionization (HR MALDI FTMS) mass spectrometry experiments were performed on an IonSpec HiResMALDI Fourier transform mass spectrometer; DHB was used as a matrix. For high-resolution mass spectral data, for compounds with molecular weight of  $\geq 2000$ , lower than 10 ppm resolution was

(24) Renslo, A. R.; Rebek, J., Jr. *Angew. Chem., Int. Ed. Engl.* **2000**, in press.

(25) Starnes, S. D.; Rudkevich, D. M.; Rebek, J., Jr. *Org. Lett.* **2000**, *2*, 1995–1998.

(26) For the recent synthesis of water-soluble self-folding cavitands, see: (a) Haino, T.; Rudkevich, D. M.; Rebek, J., Jr. *J. Am. Chem. Soc.* **1999**, *121*, 11253–11254. (b) Haino, T.; Rudkevich, D. M.; Shivanyuk, A.; Rissanen, K.; Rebek, J., Jr. *Chem. Eur. J.* **2000**, in press.

achieved.<sup>27</sup> Electrospray ionization (ESI) mass spectra were recorded on an API III Perkin-Elmer SCIEX triple quadrupole mass spectrometer.

Silica gel chromatography was performed with silica gel 60 (EM Science or Bodman, 230–400 mesh). All experiments with moisture- or air-sensitive compounds were performed in anhydrous solvents under a nitrogen atmosphere.

Molecular modeling was performed using the Amber\* force field in the MacroModel 5.5 and 6.5 program.<sup>28</sup> Molecular volumes were calculated with the GRASP program.<sup>29</sup>

**Hexaamide Cavitant (6).** Hexanitro cavitant **5**<sup>9</sup> (400 mg, 0.25 mmol) was dissolved in a mixture of toluene (60 mL) and MeOH (20 mL). To this solution was added a catalytic amount of commercial Raney nickel that had been previously washed with MeOH (2 × 5 mL). The resulting suspension was evacuated and the reaction flask was filled with H<sub>2</sub>. This operation was repeated three times and the mixture was stirred for 12 h at 40 °C under a H<sub>2</sub> atmosphere. After cooling, the Raney nickel was filtered off in a vacuum through a pad of Celite and rinsed with toluene (50 mL) and MeOH (2 × 50 mL). The filtrates were combined and evaporated under vacuum to give the hexaamino cavitant as a brown solid (355 mg, 0.25 mmol, 100%) that was taken to the next step without further purification. The hexaamino cavitant (355 mg, 0.25 mmol) was dissolved in degassed CH<sub>2</sub>Cl<sub>2</sub> (20 mL) and kept under N<sub>2</sub>. Pyridine (380 μL, 4.7 mmol) was added and the mixture was cooled to –78 °C. Propionyl chloride (204 μL, 2.4 mmol) was added slowly and the resulting solution was kept at –78 °C for 1 h. The reaction was then allowed to slowly warm to room temperature. After 14 h, the reaction mixture was diluted with CH<sub>2</sub>Cl<sub>2</sub> (30 mL) and washed with 1 N HCl (50 mL) and brine (50 mL). After drying, the organic layer was concentrated to give a residue (417 mg) that consisted of a mixture of acylated products. This residue was then dissolved in a 1:1 v/v toluene/EtOH mixture (20 mL) and to that was added NH<sub>2</sub>NH<sub>2</sub>·H<sub>2</sub>O (120 μL, 2.5 mmol). The mixture was stirred at 85 °C for 4.5 h, after which it was concentrated in a vacuum and chromatographed in silica gel, eluting with a 98:2 v/v CH<sub>2</sub>Cl<sub>2</sub>/MeOH mixture. The product **6** was obtained as a yellow solid after trituration with MeOH (55 mg, 31.0 μmol, 13%). Alternatively, hexaamide **6** was prepared in 66% yield by acylation of the corresponding hexaamino cavitant with propionyl chloride and K<sub>2</sub>CO<sub>3</sub> in EtOAc/water, 1:1, and then *O*-deacylated. Mp > 250 °C; <sup>1</sup>H NMR (benzene-*d*<sub>6</sub>, 330 K) δ 9.90 (br, 4 H), 7.68 (s, 2 H), 7.60 (s, 3 H), 7.46 (br, 1 H), 7.35 (s, 2 H), 6.98 (br, 2 H), 6.26 (t, *J* = 8 Hz, 3 H), 4.57 (br, 1 H), 2.46–2.36 (m, 20 H), 1.57–1.24 (m, 90 H), 0.97–0.93 (m, 12 H); FTIR (benzene-*d*<sub>6</sub>, cm<sup>–1</sup>) ν 3246, 2926, 2854, 1665, 1601, 1514, 1485, 1402, 1277, 1224, 937, 896; HRMS-MALDI-FTMS *m/z* 1776.1020 ([M + Na]<sup>+</sup>, calcd for C<sub>108</sub>H<sub>148</sub>N<sub>6</sub>O<sub>14</sub>Na 1776.0951).

**Dinitro Hexaamide Cavitant (7a).** A solution of hexaamide **6** (53 mg, 30.3 μmol), 1,2-difluorodinitrobenzene (12 mg, 58.8 μmol), and Et<sub>3</sub>N (42 μL, 0.30 mmol) in anhydrous DMF (10 mL) was stirred under N<sub>2</sub> for 15 h at 70 °C. The reaction mixture was cooled, and the volatiles were removed under vacuum. The residue was chromatographed on silica gel eluting with a 99:1 v/v mixture of CH<sub>2</sub>Cl<sub>2</sub>/MeOH. The dinitro product was obtained as a yellow solid after trituration with MeOH (38 mg, 19.8 μmol, 65%). Mp > 250 °C; <sup>1</sup>H NMR (benzene-*d*<sub>6</sub>, 295 K) δ 9.74 (s, 2 H), 9.70 (s, 1 H), 8.79 (s, 2 H), 7.93 (s, 2 H), 7.89 (s, 2 H), 7.86 (s, 2 H), 7.77 (s, 2 H), 7.53 (s, 2 H), 7.40 (s, 2 H), 7.31 (s, 2 H), 6.42 (t, *J* = 8 Hz, 2 H), 6.17 (t, *J* = 8 Hz, 1 H), 5.94 (t, *J* = 8 Hz, 1 H), 2.49–2.05 (m, 20 H), 1.47–1.33 (m, 72 H), 1.22–0.93 (m, 30 H); <sup>1</sup>H NMR (CDCl<sub>3</sub>, 295 K) δ 9.46 (s, 2 H), 9.32 (s, 2 H), 8.16 (s, 4 H), 7.69 (s, 2 H), 7.55 (s, 4 H), 7.36 (s, 2 H), 7.30 (s, 4 H), 7.27 (s, 2 H), 5.83–5.78 (m, 3 H), 5.60 (t, *J* = 8 Hz, 1 H), 2.57–2.40 (m, 12 H), 2.30–2.21 (m, 8 H), 1.49–1.17 (m, 90 H), 0.92 (t, *J* = 7 Hz, 12 H); <sup>13</sup>C NMR (CDCl<sub>3</sub>, 295 K) δ 173.57, 173.56, 173.55, 155.5, 154.70,

154.66, 154.1, 149.8, 149.6, 149.4, 138.6, 137.8, 136.5, 135.6, 135.4, 134.9, 128.1, 124.3, 123.7, 121.6, 121.2, 120.4, 120.3, 116.4, 115.9, 33.4, 33.3, 33.0, 32.4, 32.1, 31.9, 30.8, 30.2, 29.8, 29.7, 29.6, 29.4, 28.0, 27.9, 22.7, 14.1, 10.4, 9.8; FTIR (CH<sub>2</sub>Cl<sub>2</sub>, cm<sup>–1</sup>) ν 3409, 3249, 2927, 2854, 1666, 1599, 1540, 1514, 1483, 1070, 898, 733, 710; ESI-MS *m/z* 1919 ([M + H]<sup>+</sup>, calcd for C<sub>114</sub>H<sub>148</sub>N<sub>8</sub>O<sub>18</sub>H 1918).

**Diamino Hexaamide Cavitant (7b).** Dinitro cavitant **7a** (57 mg, 29.8 μmol) was dissolved in a mixture of toluene (15 mL) and EtOH (2 mL). A catalytic amount of commercial Raney nickel that had been previously washed with EtOH (3 × 10 mL) was added. The resulting suspension was evacuated and the reaction flask was filled with H<sub>2</sub>. This operation was repeated five times and the mixture was stirred at 40 °C under a H<sub>2</sub> atmosphere for 20 h. After cooling, the Raney nickel was filtered off in a vacuum through a pad of Celite, followed by rinsing with toluene and EtOH. The filtrates were combined and evaporated under reduced pressure to give diamine **7b** as a yellowish solid (52 mg, 28.1 μmol, 94%) which was taken to the next step without further purification.

**Molecular Container (2).** To a solution of **7b** from the previous experiment, was added terephthalaldehyde (3.7 mg, 27.6 μmol) in nitrobenzene (1 mL), the resulting solution was evacuated, and the reaction flask was filled with N<sub>2</sub>. The reaction mixture was stirred at 140 °C for 30 h. The solvent was removed under reduced pressure and the residue was purified by column chromatography (hexane/EtOAc, 4:1–2:1–1:1) to afford product **2** as a white solid (28 mg, 7.4 μmol, 52%). <sup>1</sup>H NMR (toluene-*d*<sub>8</sub>/2% DMF-*d*<sub>7</sub>/2% TFA, 295 K) δ 10.07 (s, 4 H), 9.87 (s, 4 H), 9.43 (s, 4 H), 8.09 (s, 4 H), 7.87 (s, 4 H), 7.82 (s, 4 H), 7.73 (s, 4 H), 7.63 (s, 4 H), 7.52–7.44 (m, 6 H), 7.37 (s, 4 H), 7.22 (s, 4 H), 6.29 (t, *J* = 7.8 Hz, 4 H), 6.13–6.05 (m, 4 H), 2.80–2.00 (m, 40 H), 1.70–1.20 (m, 144 H), 1.1–0.75 (m, 60 H); FTIR (toluene-*d*<sub>8</sub>, cm<sup>–1</sup>) ν 3617, 3244, 3186, 1660, 1608, 1508, 1479, 1402, 1269, 1221, 1154, 891; MALDI-MS *m/z* 3812 avg. ([M + H]<sup>+</sup>, calcd for C<sub>236</sub>H<sub>302</sub>N<sub>16</sub>O<sub>28</sub>H 3812).

**Molecular Container (3).** The crude diamine **7b** (17 mg, 9.2 μmol) was dissolved in THF (2 mL) under a N<sub>2</sub> atmosphere. 1,2,5,6-Tetraketopyracene **8**<sup>30</sup> (1.1 mg, 4.6 μmol) and glacial HOAc (20 μL) were sequentially added, and the mixture was stirred under reflux for 12 h. After cooling, the solvent was evaporated and the residue was chromatographed on a preparative thin-layer chromatography plate (silica gel, 0.5 mm) eluting with a 98:2 v/v mixture of CH<sub>2</sub>Cl<sub>2</sub>/MeOH. Two bands that correspond to the C and the S isomers were isolated (less polar band = 5.6 mg, more polar band = 4.3 mg; combined yield 9.9 mg, 2.55 μmol, 55%). Compound **3** (C-isomer): mp > 250 °C; <sup>1</sup>H NMR (toluene-*d*<sub>8</sub>, 295 K) δ 11.08 (s, 1 H, NH), 10.21 (s, 1 H, NH), 10.14 (s, 1 H, NH), 9.91 (s, 1 H, NH), 9.76 (s, 1 H, NH), 9.09 (s, 1 H, NH), 8.81 (s, 1 H, NH), 8.66 (s, 1 H, NH), 8.25 (s, 1 H, NH), 8.00 (s, 1 H, NH), 7.96–7.57 (m, 14 H), 7.33–6.79 (m, 24 H), 6.49 (m, 2 H, CH), 6.33 (m, 2 H, CH), 6.19 (m, 2 H, CH), 6.11 (m, 2 H, CH), 2.75–2.35 (m, 24 H), 2.29–1.88 (m, 16 H), 1.79–1.21 (m, 144 H), 1.06–0.91 (m, 60 H); FTIR (0.5 mM in toluene-*d*<sub>8</sub>, cm<sup>–1</sup>) ν 3244, 3180, 2926, 2854, 1664, 1512, 1483, 1330, 1275, 1229, 1183, 936, 717; MALDI-MS *m/z* 3882 avg. ([M + H]<sup>+</sup>, calcd for C<sub>242</sub>H<sub>300</sub>N<sub>16</sub>O<sub>28</sub>H 3882.2).

**Cavitant (9).** A solution of diamine **7b** (34 mg, 18.4 μmol) and terephthalaldehyde (2.6 mg, 19.3 μmol) in nitrobenzene (1 mL) was evacuated and the reaction flask was filled with N<sub>2</sub>. The reaction mixture was stirred at 140 °C for 24 h. The solvent was removed under vacuum and the residue was purified by column chromatography (hexane/EtOAc, 4:1–2:1–1:1) to afford the product as a white solid (24 mg, 12.2 μmol, 66%). <sup>1</sup>H NMR (CDCl<sub>3</sub>, 295 K) δ 12.04 (s, 1 H), 10.06 (s, 1 H), 10.03 (s, 1 H), 9.74 (s, 1 H), 9.30 (s, 1 H), 9.14 (s, 1 H), 8.86 (s, 1 H), 8.23 (s, 1 H), 7.95–7.84 (m, 5 H), 7.75 (s, 1 H), 7.70 (s, 1 H), 7.63 (s, 1 H), 7.58 (s, 1 H), 7.45 (s, 1 H), 7.44 (s, 1 H), 7.35 (s, 1 H), 7.34 (s, 1 H), 7.31–7.24 (m, 3 H), 7.22 (s, 1 H), 7.21–7.15 (m, 3 H), 5.76 (t, *J* = 8.2 Hz, 1 H), 5.73–5.61 (m, 3 H), 2.75–1.75 (m, 20 H), 1.50–1.10 (m, 90 H), 0.98–0.85 (m, 12 H); FTIR (toluene-*d*<sub>8</sub>, cm<sup>–1</sup>) ν 3234, 3186, 2928, 2851, 1703, 1665, 1608, 1512, 1484, 1407, 1269, 891; ESI-MS *m/z* 1972 ([M + H]<sup>+</sup>, calcd for C<sub>122</sub>H<sub>154</sub>N<sub>8</sub>O<sub>15</sub>H 1972).

(27) For details on high-resolution mass spectrometry, see: (a) Rose, M. E.; Johnstone, R. A. W. *Mass Spectrometry for Chemists and Biochemists*; Cambridge University Press: Cambridge, 1982. (b) Jennings, K. R.; Dolnikowski, G. G. *Methods in Enzymology*; McCloskey, J. A., Ed.; Academic Press: New York, 1990; p 37 and references therein.

(28) Mohamadi, F.; Richards, N. G.; Guida, W. C.; Liskamp, R.; Lipton, M.; Caufield, C.; Chang, G.; Hendrickson, T.; Still, W. C. *J. Comput. Chem.* **1990**, *11*, 440–467.

(29) (a) Nicholls, A.; Sharp, K. A.; Honig, B. *Proteins* **1991**, *11*, 281–296. (b) Mecozzi, S.; Rebek, J., Jr. *Chem. Eur. J.* **1998**, *4*, 1016–1022.

(30) Clayton, M. D.; Marcinow, Z.; Rabideau, P. W. *Tetrahedron Lett.* **1998**, *39*, 9127–9130.

**Cavitand (10).** To a stirred solution of diamine **7b** (90 mg, 39.5  $\mu\text{mol}$ ) and 1,2-acenaphthenequinone (21 mg, 118.5  $\mu\text{mol}$ ) in THF (20 mL) was added glacial HOAc (150  $\mu\text{L}$ ), and the resulting mixture was refluxed for 3 h. After cooling, the volatiles were removed under vacuum and the residue was purified by column chromatography eluting initially with  $\text{CH}_2\text{Cl}_2$  and then with a 99:1 v/v  $\text{CH}_2\text{Cl}_2/\text{MeOH}$  mixture. The product was obtained as a yellow solid (75 mg, 31.0  $\mu\text{mol}$ , 78%) after trituration with MeOH. Mp > 250 °C;  $^1\text{H NMR}$  (benzene- $d_6$ , 295 K)  $\delta$  10.00 (br, 2 H), 9.90 (s, 2 H), 9.62 (s, 2 H), 8.29 (s, 2 H), 7.78 (s, 2 H), 7.71 (s, 2 H), 7.68 (d,  $J = 8$  Hz, 2 H), 7.54 (t,  $J = 8$  Hz, 2 H), 7.41 (s, 2 H), 7.29 (d,  $J = 8$  Hz, 2 H), 6.87 (s, 2 H), 6.40 (t,  $J = 8$  Hz, 2 H), 6.17 (t,  $J = 8$  Hz, 1 H), 5.94 (br, 1 H), 2.64–1.25 (m, 152 H), 0.99–0.88 (m, 30 H); FTIR ( $\text{CH}_2\text{Cl}_2$ ,  $\text{cm}^{-1}$ )  $\nu$  3242, 2957, 2928, 2855, 1659, 1602, 1510, 1482, 1422, 1403, 1193, 1125, 1099, 895, 780, 678; MALDI–FTMS  $m/z$  2427 ( $[\text{M} + \text{H}]^+$ , calcd for  $\text{C}_{156}\text{H}_{214}\text{N}_8\text{O}_{14}$  2424.6).

**General Procedure for the Preparation of Amide Guests (11, 12, 16–19).** The acid chloride (1–2 equiv) was dissolved in EtOAc (2–3 mL) and added to a rapidly stirred mixture of the amine (1 equiv) and  $\text{K}_2\text{CO}_3$  (2 equiv) in a 1:1 EtOAc/ $\text{H}_2\text{O}$  mixture (50 mL). After 3 h, the mixture was diluted with EtOAc (100 mL) and the organic layer was separated, washed with brine, dried over  $\text{MgSO}_4$ , and filtered. The solvent was removed in a vacuum to give amides **11**, **12**, and **15–18** as white solids in 56–90% yields. 4-(4-Methylphenyl)benzoic acid was prepared by the literature protocol<sup>31</sup> and converted into the corresponding acid chloride by refluxing in thionyl chloride for 3 h under  $\text{N}_2$ .

***N*-(Cyclohexyl)-*n*-octanoylamide (11).** Mp 74–75 °C;  $^1\text{H NMR}$   $\delta$  5.37 (br s, 1H, NH), 3.77 (m, 1H, CH-cycl), 2.13 (t,  $J = 7.6$  Hz, 2H, C(O)CH<sub>2</sub>), 1.91 (dd,  $J = 12.3, 3.2$  Hz, 2 H, CH<sub>2</sub>), 1.71–1.09 (m, 18 H, CH<sub>2</sub>), 0.88 (t,  $J = 6.9$  Hz, 3 H, CH<sub>3</sub>);  $^{13}\text{C NMR}$   $\delta$  172.6, 48.4, 37.5, 33.7, 32.1, 29.6, 29.4, 26.3, 25.9, 25.3, 23.0, 14.5; IR  $\nu$  3292, 2919, 2852, 1633, 1548, 1471, 1443, 1248, 1210, 967, 890, 719, 610, 562; HRMS–FAB  $m/z$  226.2170 ( $[\text{M} + \text{H}]^+$ , calcd for  $\text{C}_{14}\text{H}_{28}\text{NO}$  226.2171).

***N*-(Cyclohexyl)-4-(4-methylphenyl)benzamide (12).** Mp 223–224 °C;  $^1\text{H NMR}$  (300 MHz,  $\text{CDCl}_3$ , 295 K)  $\delta$  7.82 (d,  $J = 8.2$  Hz, 2H), 7.63 (d,  $J = 8.2$  Hz, 2 H), 7.51 (d,  $J = 8.2$  Hz, 2 H), 7.28 (d,  $J = 8.2$  Hz, 2 H), 6.04 (d,  $J = 7.6$  Hz, 1 H), 4.06–3.96 (m, 1 H), 2.41 (s, 3 H), 2.08–2.04 (m, 2 H), 1.80–1.74 (m, 2 H), 1.70–1.65 (m, 2 H), 1.47–1.40 (m, 2 H), 1.30–1.20 (m, 2 H);  $^{13}\text{C NMR}$  (75 MHz,  $\text{CDCl}_3$ , 295 K)  $\delta$  166.8, 144.4, 138.3, 137.6, 133.8, 130.0, 127.7, 127.3, 127.2, 49.0, 33.7, 26.0, 25.3, 21.5; HRMS–MALDI–FTMS  $m/z$  294.1843 ( $[\text{M} + \text{H}]^+$ , calcd for  $\text{C}_{20}\text{H}_{23}\text{NOH}$  294.1852).

***N*-(1-Adamantyl)-*p*-methylcinnamamide (15).** Mp 136–137 °C;  $^1\text{H NMR}$  ( $\text{CDCl}_3$ , 295 K)  $\delta$  7.57 (d,  $J = 16$  Hz, 1 H), 7.36 (d,  $J = 8$  Hz, 2 H), 7.16 (d,  $J = 8$  Hz, 2 H), 6.36 (d,  $J = 16$  Hz, 1 H), 5.41 (br s, 1 H), 2.36 (s, 3 H), 2.1, 1.7 (2  $\times$  m, 15 H);  $^{13}\text{C NMR}$  ( $\text{CDCl}_3$ , 295 K)  $\delta$  165.5, 140.5, 140.0, 132.7, 129.9, 128.1, 121.5, 52.5, 42.1, 36.8, 29.8, 21.8; HRMS–MALDI–FTMS  $m/z$  318.1820 ( $[\text{M} + \text{Na}]^+$ , calcd for  $\text{C}_{20}\text{H}_{25}\text{NONa}$  318.1828).

***N*-(1-Adamantyl)-*n*-octanoylamide (16).** Mp 68–69 °C (MeCN);  $^1\text{H NMR}$  (300 MHz,  $\text{CD}_2\text{Cl}_2$ , 295 K)  $\delta$  5.12 (s, 1 H), 2.07–2.00 (m, 4 H), 1.98–1.91 (m, 6 H), 1.70–1.62 (m, 6 H), 1.61–1.50 (m, 3 H), 1.34–1.21 (m, 8 H), 0.87 (t, 7.0 Hz, 3 H);  $^{13}\text{C NMR}$  (75 MHz,  $\text{CD}_2\text{Cl}_2$ , 295 K)  $\delta$  172.3, 51.8, 42.0, 38.1, 36.7, 32.1, 30.0, 29.5, 29.4, 23.0, 14.2; ESI-MS  $m/z$  278 ( $[\text{M} + \text{H}]^+$ , calcd for  $\text{C}_{18}\text{H}_{31}\text{NOH}$  278).

***N*-(1-Adamantyl)-4-(4-methylphenyl)benzamide (17).** Mp 167–169 °C (cyclohexane);  $^1\text{H NMR}$  ( $\text{CDCl}_3$ , 295 K)  $\delta$  7.79 (d,  $J = 8$  Hz, 2 H), 7.63 (d,  $J = 8$  Hz, 2 H), 7.52 (d,  $J = 8$  Hz, 2 H), 7.28 (d,  $J = 8$  Hz, 2 H), 5.88 (s, 1 H), 2.42 (s, 3 H), 2.16 (s, 9 H), 1.75 (dd,  $J = 13$  Hz,  $\Delta\nu = 20$  Hz, 6 H);  $^{13}\text{C NMR}$  ( $\text{CDCl}_3$ , 295 K)  $\delta$  166.33, 143.71, 137.76, 137.16, 134.33, 129.75, 127.16, 126.96, 126.83, 52.26, 41.72, 36.34, 29.50, 21.10; FTIR ( $\text{CDCl}_3$ ,  $\text{cm}^{-1}$ )  $\nu$  3434, 3029, 2911, 2852, 1906, 1659, 1610, 1530, 1512, 1489, 1301, 1248, 1088, 859, 817; HRMS–MALDI–FTMS  $m/z$  346.2149 ( $[\text{M} + \text{H}]^+$ , calcd for  $\text{C}_{24}\text{H}_{27}\text{NOH}$  346.2165).

**4-(4-Ethylphenyl)benzoic Acid.** A solution of 4-ethylphenylmagnesium bromide, prepared from bromo-4-ethylbenzene (1.38 mL, 10.0 mmol), magnesium turnings (267 mg, 11.0 mmol), and anhydrous  $\text{Et}_2\text{O}$  (10 mL), was added dropwise to a rapidly stirring solution of trimethyl borate (280  $\mu\text{L}$ , 2.5 mmol) and anhydrous  $\text{Et}_2\text{O}$  (3 mL) over a 45 min period. The resulting white suspension refluxed for 30 min, and then a mixture of sodium hydroxide (1.25 g, 31.3 mmol), 4-iodobenzoic acid (1.55 g, 6.3 mmol),  $\text{PdCl}_2$  (11 mg, 62.5  $\mu\text{mol}$ ), and water (45 mL) was added slowly. The resulting mixture was refluxed for another hour and then was extracted with  $\text{Et}_2\text{O}$  (2  $\times$  100 mL). The combined organic extracts were washed with brine, dried over  $\text{MgSO}_4$ , and filtered. The solvent was removed in a vacuum and the resulting white solid was purified by column chromatography, eluting with a 2:1 v/v mixture of hexanes/ $\text{EtOAc}$ . The product was obtained as a white solid after recrystallization from  $\text{EtOH}$  (423 mg, 1.87 mmol, 30%).  $^1\text{H NMR}$  (acetone- $d_6$ , 295 K)  $\delta$  8.10 (d,  $J = 8$  Hz, 2 H), 7.77 (d,  $J = 8$  Hz, 2 H), 7.65 (d,  $J = 8$  Hz, 2 H), 7.34 (d,  $J = 8$  Hz, 2 H), 2.69 (q,  $J = 7$  Hz, 2 H), 1.26 (t,  $J = 7$  Hz, 3 H);  $^{13}\text{C NMR}$  (acetone- $d_6$ , 295 K)  $\delta$  167.6, 146.2, 145.4, 138.1, 131.1, 130.1, 129.5, 128.0, 127.6, 29.1, 16.1.

***N*-(1-Adamantyl)-4-(4-ethylphenyl)benzamide (18).** Mp 198–200 °C (cyclohexane);  $^1\text{H NMR}$  ( $\text{CDCl}_3$ , 295 K)  $\delta$  7.79 (d,  $J = 8$  Hz, 2 H), 7.63 (d,  $J = 8$  Hz, 2 H), 7.55 (d,  $J = 8$  Hz, 2 H), 7.31 (d,  $J = 8$  Hz, 2 H), 5.87 (s, 1 H), 2.72 (q,  $J = 8$  Hz, 2 H), 2.16 (s, 9 H), 1.75 (dd,  $J = 13$  Hz,  $\Delta\nu = 20$  Hz, 6 H), 1.30 (t,  $J = 8$  Hz, 3 H);  $^{13}\text{C NMR}$  ( $\text{CDCl}_3$ , 295 K)  $\delta$  166.4, 144.1, 143.8, 137.4, 134.3, 128.4, 127.2, 127.1, 126.9, 52.3, 41.7, 36.4, 29.5, 28.5, 15.6; FTIR ( $\text{CDCl}_3$ ,  $\text{cm}^{-1}$ )  $\nu$  3434, 3028, 2911, 2852, 1906, 1657, 1610, 1529, 1513, 1490, 1302, 1248, 1005, 829; HRMS–MALDI–FTMS  $m/z$  360.2338 ( $[\text{M} + \text{H}]^+$ , calcd for  $\text{C}_{25}\text{H}_{29}\text{NOH}$  360.2322).

***N*-(1-Adamantyl)-*p*-(*n*-heptyl)benzamide (19).** Mp 87–88 °C;  $^1\text{H NMR}$  (600 MHz,  $\text{CDCl}_3$ , 295 K)  $\delta$  7.64 (d,  $J = 8$  Hz, 2 H), 7.23 (d,  $J = 8$  Hz, 2 H), 5.84 (br s, 1 H), 2.63 (2  $\times$  d,  $J = 7.8$  Hz, 2 H), 2.1, 1.75, 1.6, 1.35, 1.3 (5  $\times$  m, 25 H), 0.89 (t,  $J = 7.5$  Hz, 3 H);  $^{13}\text{C NMR}$  ( $\text{CDCl}_3$ , 295 K)  $\delta$  167.0, 146.7, 143.8, 133.8, 128.8, 127.1, 52.5, 42.1, 36.8, 36.2, 32.2, 31.7, 29.9, 29.55, 29.52, 23.0, 14.5; HRMS–MALDI–FTMS  $m/z$  354.2800 ( $[\text{M} + \text{H}]^+$ , calcd for  $\text{C}_{24}\text{H}_{35}\text{NOH}$  354.2791).

**Acknowledgment.** We are grateful for financial support from the Skaggs Research Foundation and the National Institutes of Health. U.L. thanks Alexander von Humboldt Stiftung, Feodor-Lynen programm for the scholarship. Drs. Laura Pasternack and Dee-Hua Huang are sincerely acknowledged for their assistance with the 2D NMR experiments. We also grateful to Prof. Göran Hilmersson of Göteborg University and to Drs. Adam R. Renslo and Lubomir Sebo for experimental advice.

(31) Bumagin, N. A.; Bykov, V. V. *Tetrahedron* **1997**, *53*, 14437–14450.